Contamination dose from photoneutron processes in bodily tissues during therapeutic radiation delivery

F. Difilippo
Radiation Transport and Physics Group, Oak Ridge National Laboratory, Oak Ridge, Tennessee 37831-6363

L. Papiez[a] and V. Moskvin
Department of Radiation Oncology, Indiana University, Indianapolis, Indiana 46202-5289

D. Peplow
Radiation Transport and Physics Group, Oak Ridge National Laboratory, Oak Ridge, Tennessee 37831-6363

C. DesRosiers
Department of Radiation Oncology, Indiana University, Indianapolis, Indiana 46202-5289

J. Johnson
Radiation Transport and Physics Group, Oak Ridge National Laboratory, Oak Ridge, Tennessee 37831-6363

R. Timmerman and M. Randall
Department of Radiation Oncology, Indiana University, Indianapolis, Indiana 46202-5289

R. Lillie
Radiation Transport and Physics Group, Oak Ridge National Laboratory Oak Ridge, Tennessee 37831-6363

(Received 21 October 2002; accepted for publication 31 July 2003; published 26 September 2003)

Dose to the total body from induced radiation resulting from primary exposure to radiotherapeutic beams is not detailed in routine treatment planning though this information is potentially important for better estimates of health risks including secondary cancers. This information can also allow better management of patient treatment logistics, suggesting better timing, sequencing, and conduct of treatment. Monte Carlo simulations capable of taking into account all interactions contributing to the dose to the total body, including neutron scattering and induced radioactivity, provide the most versatile and accurate tool for investigating these effects. MCNPX code version 2.2.6 with full IAEA library of photoneutron cross sections is particularly suited to trace not only photoneutrons but also protons and heavy ion particles that result from photoneutron interactions. Specifically, the MCNPX code is applied here to the problem of dose calculations in traditional (non-IMRT) photon beam therapy. Points of calculation are located in the head, where the primary irradiation has been directed, but also in the superior portion of the torso of the ORNL Mathematical Human Phantom. We calculated dose contributions from neutrons, protons, deutrons, tritons and He-3 that are produced at the time of photoneutron interactions in the body and that would not have been accounted for by conventional radiation oncology dosimetry. © *2003 American Association of Physicists in Medicine.* [DOI: 10.1118/1.1612947]

Key words: photoneutron, neutron dosimetry, whole body dose, dose from heavy charged particles, Monte Carlo simulation, internal dosimetry, MCNPX

INTRODUCTION

In radiation therapy, delivery of dose occurs primarily in specific, intentionally exposed regions of the body. These regions include the target and volumes of tissue juxtaposed along the path of radiation beams. The dosimetric representations of such radiation therapy treatments are generally limited to these same regions plus some volumes in their vicinity (e.g., volumes exposed to radiation ''transferred'' by blocks or collimator multileaves). Dose calculations are not explicitly reported to other regions of the patient body, especially those far removed from the primary beams. These unaccounted dose contributions include leakage radiation, dose from photoneutrons and dose from induced radioactivity originating in the patient's body, in radiation equipment and in treatment accessories.

The main source of the ''contamination'' radiation responsible for doses in body tissues outside of primary beams is the scattered radiation from the accelerator head. Measurements quantifying the dose from this radiation source vary considerably, but indicate that resulting dose is less than 2.5% of prescribed dose[2] and show strong dependence on treatment conditions and accelerator design.[2] Therefore, any comprehensive evaluation of the total contamination dose to a patient's body will have to include the scatter radiation,

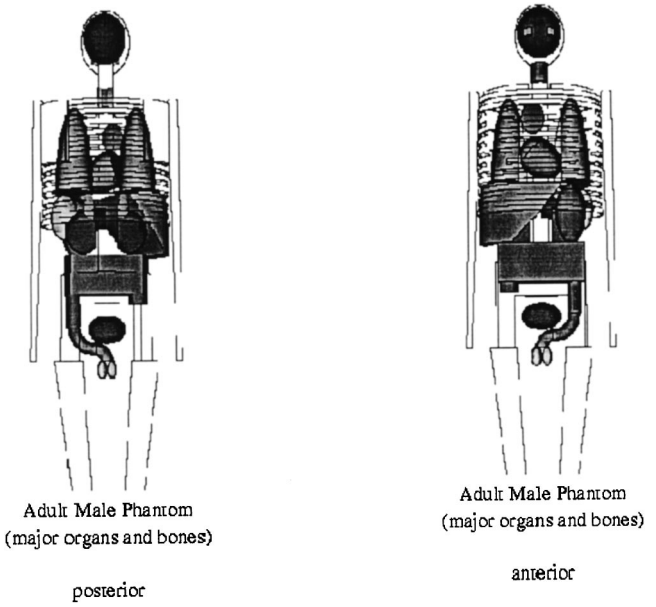

FIG. 1. The ORNL adult male human phantom visible from anterior and posterior.

including secondary neutrons, from the accelerator head. We are currently involved in investigating this elaborate problem and expect to present relevant results in the near future. However, in this paper we aim to present results on partial dose contamination that originates from interactions in the primary exposed volumes of tissues of the patient's body only. We calculate dose contributions from neutrons, protons, deuterons, tritons and He-3 that are produced at the time of photoneutron interactions in the body and that would not have been accounted for by conventional radiation oncology dosimetry.

Specifically, this paper is devoted to the study of photoneutron generated particles from primary photon beams. The rationale to separate study of photoneutron dose from interactions originating in the human body from photoneutron dose from interactions originating in the accelerator head is the distinct radiobiological effect of these two doses. Generally, neutron production in the human body will be accompanied by secondary short range heavy charged particles[3] whose relative biological effectiveness (RBE) factor is large.[4] In contrast, the neutron production in the accelerator head will contribute dose to patients from neutrons that may reach the body, but will not contribute secondary short range heavy charged particles since they will be absorbed in machine head and shielding. Furthermore, when doses from both types of neutron sources are scored together, it may not be possible to investigate their distinct contributions with different RBE characteristics.[5,6]

METHODS

To exploit the potential of MCNPX code in radiotherapy applications the joint project between Radiation Transport and Physics Group of Oak Ridge National Laboratory and the Department of Radiation Oncology of Indiana University has been initiated. The goal of the project is to design a comprehensive set of MCNPX simulations, and to collect and interpret data of these simulations for the purpose of evaluating all therapeutic and radiation protection risks associated with whole body dose and its neutron/heavy particle component.

This paper is devoted to the preliminary study in which, assuming the simplified geometry of the radiotherapeutic source of photons, evaluation of the neutron flux and the photoneutron dose in a patient body accumulated during a photon beam therapy is investigated. The goal of this investigation is to study photoneutron dose from interactions originating in human body only. To be consistent with the above objective we initiate simulations without taking into account accelerator beam lines. Instead we assume a pure and straightforward geometry for the initial beam, free of any contamination but characterized by realistic, clinical beam spectra. As far as beam spectra are concerned we use data for high-energy photon beams (18 MV–Varian Clinac HE and 25 MV–Elekta SL25) that are available in physical literature.[7,8] As far as beam geometry is concerned we assume symmetrical distribution of particles' tracks and directions that closely represent the real distributions of incoming patient body photon rays. We presume that all photons originate from a point source and that they are ideally collimated so that their straight-line tracks form a pyramid that, at some distance L (at the surface of the phantom), defines a square in the plane perpendicular to the beam's central axis. Points that represent crossings of propagating particles with the plane perpendicular to the central axis are distributed uniformly in the square. Moreover, we assume that when crossing the above plane particles travel strictly along rays emanating from the point source. Thus no scattering of primary photons happens before particles come to the square discussed above and the distribution of particles' directions at any point of the square is (Dirac's) delta function concentrated on the angle defined by the direction of ray originating at point source and crossing plane at point of interest.

The above-described beam of photons has been directed in our simulations towards a humanoid model (ORNL Mathematical phantom;[1] see Fig. 1. Table I, and Table II). The humanoid model accurately reflects proportions of isotopic abundances in various human tissues (Tables III, IV, and V). The MCNPX Monte Carlo dose calculations presented in this work seem to be the first Monte Carlo simulations in which truly representative model of the human body, as far as photonuclear interactions are concerned, has been investigated. Particular examples of these computations are provided for the treatment of the brain by typical AP/PA plus left

TABLE I. Mathematical phantom distribution of materials. Three kinds of tissue are considered: lung, tissue, and bone.

	Lung	Tissue	Bone	Body total
Volume (cm^3)	3378.000	59 493.948	7045.260	69 917.208
Density (g/cm^3)	0.2958	0.9869	1.4862	
Mass (g)	999.212	58 714.577	10 470.665	70 184.455

TABLE II. Weight factors for elements in lung, muscles and bone tissues used in mathematical phantom.

	Lung	Tissue	Bone
H	0.1021	0.1047	0.0704
C	0.1001	0.2302	0.2279
N	0.0280	0.0234	0.0387
O	0.7596	0.6321	0.4856
Na	0.0019	0.0013	0.0032
Mg	0.0	0.0002	0.0011
P	0.0008	0.0024	0.0694
S	0.0023	0.0022	0.0017
Cl	0.0027	0.0014	0.0014
K	0.0020	0.0021	0.0015
Ca	0.0001	0.0	0.0991
Fe	0.0004	0.0	0.0

and right laterals (each beam is 10×10 cm at 100 cm SAD), and for the purpose of developing some intuitive assessment of dose values in the simplest case, also for the case of single lateral field. To this end photon beams with characteristics defined above are set on the humanoid phantom and their penetration from the surface of the body inside is simulated with the MCNPX (version 2.2.6) code.

Simulations have been performed to provide answers for typical questions of dose contamination from photoneutron interactions within patient body. Doses reported have been scored as averages over various organs. Therefore switching off electron transport may be justifiable for most simulations of this type. In the case of OFF electron transport, secondary electrons are forced to deposit their energy in the spatial point where they are generated. The first case considered was a simple simulation of treatment with single photon beam directed towards Mathematical Phantom head. Doses from different types of particles in Gy for distinct parts of phantom head for single 25 MV beam (Elekta SL25) are reported in Table VI. $5E+06$ primary photons were simulated.

The second treatment considered was a simulation of clinically realistic beam arrangement of four fields, AP/PA and right/left laterals. Two cases of treatment, one for beams of energies 25 MV (Elekta SL25) and the second one for beams of energies 18 MV (Varian Clinac HE) have been simulated. Prescribed dose is also equal to 2 Gy at isocenter. Reported data have been scored for transport with ''switched ON'' electron tracing only. $5E+07$ primary photons were simulated. For the case of the second treatment the important parameters of contamination dose evaluation were ratios of doses from different types of particles to photon doses obtained for various organs and body parts of the upper part of the phantom torso. Doses for the second treatment are reported in Tables VII and VIII. Relative uncertainties for these are also included in tables.

TABLE III. Abundant isotopes in the brain with (γ,n) thresholds below 15 MeV.

Isotope	% natural abundance	Threshold (MeV)
N-14	99.63	10.55
Na-23	100.	12.42
P-31	100.	12.3
Cl-35	75.77	12.65
K-39	93.26	13.08

TABLE IV. Rare isotopes in the brain with lower (γ,n) thresholds.

Isotope	% natural abundance	Threshold (MeV)	Gram in body
H-2	0.015	2.2	2.1
C-13	1.1	4.95	190.6
O-17	0.038	4.14	17.3
O-18	0.2	8.04	96.65
Mg-25	10	7.33	2.39
S-33	0.75	8.64	1.15
K-40	0.012	7.8	0.017

RESULTS

Doses from photons and doses from secondary particles originating in photonuclear reactions in tissue for brain treatments have been compiled for various areas of the head and torso in our report. This has been done for regions directly exposed to the primary beam of photons and also for regions that lay at some distance from the primary beam trajectories. In particular, doses in sensitive areas of face and eye that are not exposed to primary irradiation have been calculated, as well as doses to the thyroid, lung and ribs. The fraction of neutron dose relative to photon dose for particles that originate from interactions in the human body has been found to increase generally with the distance from regions directly exposed to primary beams. This increase may be even more significant as far as ratio of dose equivalent is concerned due to relative increase with the distance of low energy neutrons associated with high dose equivalent factor.[4–6] The main factor responsible for this somewhat unexpected behavior of dose ratios from scattered neutrons and scattered photons is more isotropic property of neutron scattering than photon scattering. In consequence, we observe that the relative importance of neutrons as a contributor to the total body dose equivalent in radiation therapy may need upward adjustment. Still the overall contribution of dose equivalent from neutrons produced in the patient body remains, according to our calculations (in regions not exposed to direct irradiation) at

TABLE V. Ranking of the isotopes for production of neutrons in the brain. Column absolute represents amount of neutrons generated per incident photon.

Isotope	Absolute	%
O-17	$2.600E-06$	45.61
S-32	$1.200E-06$	21.05
N-14	$7.000E-07$	12.28
Na-23	$4.000E-07$	7.02
C-12	$2.000E-07$	3.51
O-18	$2.000E-07$	3.51
K-40	$2.000E-07$	3.51
S-33	$1.000E-07$	1.75
N-15	$1.000E-07$	1.75

TABLE VI. Doses from different types of particles in Gy for distinct parts of phantom head for single 25 MV beam (Elekta SL25). Prescribed dose is equal to 2 Gy at isocenter. Data are given for transport with ''switched ON'' and ''switched OFF'' secondary electron tracing in MCNPX. In the case of ''switched OFF'' electron transport, secondary electrons are forced to deposit their energy in the spatial point where they were generated. $5E+06$ primary photons were simulated.

		Dose (Gy)	
Particle	Organ	Secondary *e* transport ON	Secondary *e* transport OFF
Gamma	Face	$5.359E-02$ (0.03)	$5.370E-02$ (0.03)
	Brain	$2.0000E+00$ (0.03)	$2.001E+00$ (0.03)
	Skull	$4.725E-01$ (0.03)	$4.730E-01$ (0.03)
	2 eyes	$1.042E-02$ (0.03)	$1.028E-02$ (0.03)
Neutrons	Face	$2.058E-06$ (0.20)	$2.436E-06$ (0.18)
	Brain	$1.955E-05$ (0.13)	$1.698E-05$ (0.12)
	Skull	$1.050E-05$ (0.12)	$1.108E-05$ (0.13)
	2 eyes	$9.709E-08$ (0.70)	$6.381E-08$ (0.90)
Protons	Face	$3.842E-06$ (0.05)	$3.825E-06$ (0.05)
	Brain	$1.688E-04$ (0.08)	$1.688E-04$ (0.08)
	Skull	$8.730E-05$ (0.13)	$8.731E-05$ (0.14)
	2 eyes		
Deuterons	Face	$2.350E-09$ (0.58)	$2.350E-09$ (0.58)
	Brain	$3.362E-07$ (0.15)	$3.362E-07$ (0.14)
	Skull	$7.668E-08$ (0.60)	$7.668E-08$ (0.51)
	2 eyes		
Alphas	Face	$1.384E-06$ (0.08)	$1.386E-06$ (0.09)
	Brain	$5.472E-05$ (0.02)	$5.463E-05$ (0.04)
	Skull	$2.316E-05$ (0.03)	$2.299E-05$ (0.03)
	2 eyes		

TABLE VII. Doses from different types of particles in Gy for distinct parts of phantom head for four-field box beam treatment with 25 MV beam (Elekta SL25) and 18 MV beam (Varian Clinac HE). Prescribed dose is equal to 2 Gy at isocenter. Data are given for transport with ''switched ON'' electron tracing. $5E+07$ primary photons were simulated.

		Dose (Gy)	
Particle	Organ	Elekta (25 MV)	Varian (18 MeV)
Gamma	Face	$4.536E-02$ (0.01)	$4.666E-02$ (0.01)
	Brain	$2.000E+00$ (0.01)	$2.000E+00$ (0.01)
	Skull	$3.920E-01$ (0.01)	$3.927E-01$ (0.01)
	Left eye	$3.705E-02$ (0.01)	$4.211E-02$ (0.01)
	Right eye	$3.701E-02$ (0.01)	$4.238E-02$ (0.01)
Neutrons	Face	$1.988E-06$ (0.06)	$1.217E-06$ (0.09)
	Brain	$1.945E-05$ (0.04)	$1.154E-05$ (0.05)
	Skull	$8.382E-06$ (0.04)	$5.418E-06$ (0.05)
	Left eye	$2.031E-05$ (0.31)	$8.536E-06$ (0.53)
	Right eye	$3.390E-06$ (0.57)	$4.235E-06$ (0.56)
Protons	Face	$3.533E-06$ (0.01)	$2.134E-06$ (0.02)
	Brain	$1.704E-04$ (0.01)	$1.055E-04$ (0.01)
	Skull	$6.966E-05$ (0.04)	$4.185E-05$ (0.07)
	Left eye	$5.636E-08$ (0.68)	$1.751E-08$ (0.57)
	Right eye	$7.224E-09$ (0.58)	$9.236E-09$ (0.83)
Deuterons	Face	$1.126E-08$ (0.21)	$3.534E-09$ (0.25)
	Brain	$3.934E-07$ (0.04)	$1.851E-07$ (0.06)
	Skull	$1.126E-07$ (0.12)	$5.668E-08$ (0.19)
	Left eye		
	Right eye		
Alphas	Face	$1.061E-06$ (0.03)	$7.252E-07$ (0.03)
	Brain	$5.536E-05$ (0.01)	$3.685E-05$ (0.01)
	Skull	$1.917E-05$ (0.01)	$1.247E-05$ (0.01)
	Left eye		
	Left eye		

TABLE VIII. Ratio of doses from different types of particles to photon doses for various organs and body parts. Relative uncertainties are included in parenthesis. (*) mark means that statistical error was not defined due to low count of events in simulation. Photon dose in Gy is listed in right column for a case of 2 Gy dose at isocenter for irradiation by single 25 MV beam (Elekta SL25). The relative uncertainty is 0.01 with $1E+08$ primary photon histories.

	Ratio of the dose for various particles to the photon dose				Photon dose, Gy
	Neutron	Proton	Deuteron	Alpha	
Face	$4.03E-05$ (0.05)	$7.77E-05$ (0.01)	$2.38E-07$ (0.13)	$2.46E-05$ (0.02)	$7.925E-02$
Brain	$1.03E-05$ (0.03)	$\sim 8.45E-05$ (*)	$1.87E-07$ (0.03)	$\sim 2.75E-05$ (*)	$2.000E+00$
Skull	$2.07E-05$ (0.03)	$\sim 1.80E-04$ (*)	$2.70E-07$ (0.1)	$4.88E-05$ (0.01)	$4.094E-01$
Left eye	$4.34E-04$ (0.58)				$1.362E-05$
Right eye	$7.53E-05$ (0.53)	$4.64E-09$ (0.87)			$2.528E-05$
Thyroid	$1.85E-04$ (0.55)	$2.11E-09$ (0.39)			$4.793E-05$
Thymus	$1.66E-06$ (0.99)	$7.58E-08$ (0.99)			$8.302E-06$
Left lung	$4.98E-04$ (0.45)	$1.36E-09$ (0.35)			$8.208E-05$
Right lung	$8.98E-05$ (0.54)	$4.04E-09$ (0.47)			$1.413E-04$
Spine	$1.54E-04$ (0.23)	$3.71E-08$ (0.96)			$7.094E-04$
Left scapulae	$2.00E-04$ (0.57)	$3.90E-09$ (0.56)			$3.283E-05$
Right scapulae	$1.14E-05$ (0.64)	$2.02E-10$ (0.76)			$8.434E-05$
Left clavicle	$7.23E-04$ (0.46)	$2.49E-09$ (0.99)			$2.736E-05$
Right clavicle	$2.81E-04$ (0.41)	$2.11E-09$ (0.75)			$6.208E-05$
Upper torso	$1.71E-04$ (0.13)	$4.65E-06$ (0.13)	$1.25E-07$ (0.71)		$4.151E-03$
Top rib	$2.97E-07$ (0.99)	$4.35E-10$ (0.99)			$2.057E-05$
Second rib	$1.59E-04$ (0.78)	$1.26E-09$ (0.79)			$3.019E-05$
Third rib	$5.46E-05$ (0.58)	$5.60E-07$ (0.99)			$4.547E-05$
Fourth rib	$1.73E-04$ (0.32)	$1.79E-09$ (0.62)			$7.132E-05$

least one order of magnitude lower than the dose equivalent from gamma (γ) radiation. Please, notice that the above comparison is for the dose equivalent and not the dose itself (as presented in our tables) where the difference between neutron and photon dose component is evaluated as varying by 3 to 4 orders of magnitude.

It is interesting to note that the dose in tissue exposed to primary beam channels from some of the charged particles (e.g., protons and alphas) produced in photonuclear reactions (see Tables VII and VIII) is higher than the dose deposited by neutrons produced in these reactions. This, in turn, shows that for (γ-n) threshold reactions, charged particles are emitted inside the human body during routine therapeutic irradiations more often than it is generally perceived.

DISCUSSION

Dose from secondary and induced sources are unintentional and are generally of low levels. Still, their biological effect may have unintended negative consequences, especially in vulnerable patient populations like children and women of child bearing potential. Ideally, these ''contamination'' sources of radiation would be accounted for or reasonably quantified for complete understanding of dose deposition.

Secondary particles subsequent to photoneutron reactions inside a patient's body provide certain contribution to the whole body dose, and their high value of RBE increases the overall risks associated with the whole body exposure. Notwithstanding the fact that this dose is miniscule by comparison to primary dose to target this dose is not negligible from the point of view of long term medical consequence.[4–6]

There are two other factors that make investigations of contamination dose especially relevant. Both are related to potential increase of dose to the whole body during radiotherapy treatments delivered with the most modern equipment. First, the total body dose increases (quite proportionally due to the leakage radiation and photoneutron contamination) with increasing number of monitor units utilized during MLC IMRT treatments. Second, MLC IMRT capable accelerators have more complex treatment head design, with more scattering elements than a conventional, pre-MLC treatment machine. The work by Gudowska[9,10] shows that the increase in accelerator head complexity leads to a considerable enhancement of the neutron flux. In light of all these considerations it seems essential to look for tools capable of providing accurate, reliable and fairly economical determination of dose to the whole patient body for all types of external beam radiation treatments. This paper demonstrates that specific questions related to contamination dose can be treated successfully by Monte Carlo codes and indicates that complete evaluation of contamination doses can be provided through this approach. Moreover, this methodology does not require specialized equipment for time consuming measurements and is also flexible for various possible scenarios of radiation utilization in clinic.[11,12] Until recently, however, generic codes suitable for these applications have not been available and development of dedicated to this type of dose modeling software was a task beyond means of any radiation therapy department. Fortunately, the latest compilation of the full IAEA library of photoneutron cross sections,[13] and its integration with the MCNPX Monte Carlo code,[14] created the tool that is very well suited for the purpose. This computational device allows modeling, of the photoneutron and induced radioactivity components to dose at any region of the patient body and allows also evaluating risks of dose exposure to medical personnel involved in ra-

diation therapy treatments. In contrast, measurements of doses from contaminating radiation can be intricate. Moreover, the empirical collection of data is not very useful in situations when new equipment is introduced and new use of the equipment (new treatment techniques) is proposed. In such situations it is desirable to know the impact of these innovations on risks involved beforehand while empirical data are available after implementation only.[15]

CONCLUSIONS

It has been demonstrated in this paper that MCNPX code is an appropriate tool for calculating comprehensive data on the photonuclear component of the dose distribution in photon radiation therapy. In particular, it has been shown that MCNPX can be used for evaluation of dose from a variety of particles produced in photo-nuclear reactions inside patient body. This dose has not generally been calculated before for radiation therapy treatments and it can potentially be of consequence due to high LET values of some of the particles that contribute to this contamination.

The geometry of the human body can be closely modeled for the purpose of these dose calculations by ORNL Mathematical Human Phantom. Taking into account the flexibility of geometrical modeling in the MCNPX code, as well as modeling of beam shaping devices, it can be expected that the same code can be used successfully for modeling of total dose contribution from contaminating radiation originating in MLC equipped machine heads as well as from patient bodies and all equipment inside the treatment room. This expectation indicates the direction of future research in the area of complete and accurate evaluation of contaminating doses in radiotherapy treatments. This research requires MCNPX code capabilities in simulating entire beam lines of clinical, linear accelerators, simulating the formation of radioactive sources in all equipment and patient and calculate subsequently contaminating dose to the whole patient as well as to personnel involved in delivery of radiotherapy treatments.

[a]Electronic mail: lpapiez@iupui.edu

[1] M. Cristy, ''Mathematical phantoms representing children of various ages for use in estimates of internal dose,'' U.S. Nuclear Regulatory Commission Report No. NUREG/CR-1159 (also Oak Ridge National Laboratory Report No. ORNL/NUREG/TM-367) (1980).

[2] L. Cozzi, F. M. Buffa, and A. Fogliata, ''Dosimetric features of linac head and phantom scattered radiation outside the clinical beam: experimental measurements and comparison with treatment planning system calculations,'' Radiother. Oncol. **58**, 193–200 (2001).

[3] V. G. Nedoresov and Yu. H. Ranuk, *Photo-division of Nuclei Above Giant Resonance*, 1st ed. (Naukova Dumka, Kiev, 1989) (in Russian).

[4] E. J. Hall, *Radiobiology for the Radiologist*, 4th ed. (Lippincott Williams & Wilkins, New York, 1993).

[5] A. M. Kellerer and L. Walsh, ''Solid cancer risk coefficient for fast neutrons in terms of effective dose,'' Radiat. Res. **158**, 61–68 (2002).

[6] A. M. Kellerer and L. Walsh, ''Risk estimation for fast neutrons with regard to solid cancer,'' Radiat. Res. **156**, 708–717 (2001).

[7] D. Sheikh-Bagheri and D. W. O. Rogers, ''Monte Carlo calculation of nine megavoltage photon beam spectra using the BEAM code,'' Med. Phys. **29**, 391–402 (2002).

[8] R. Mohan, C. Chui, and L. Lidofsky, ''Energy and angular distributions of photons from medical linear accelerators,'' Med. Phys. **12**, 592–597 (1985).

[9] I. Gudowska, ''Measurements of the neutron absorbed dose from medical accelerators,'' Internal Report, Dept. of Radiation Physics, The Karolinska Institute, Stockholm, RI 1984-04, pp. 1–87, 1984.

[10] I. Gudowska and A. Brahme, ''Neutron radiation from high-energy x-ray medical accelerators,'' Nukleonika **41**, 99–112 (1996).

[11] V. Moskvin, L. Papiez, C. DesRosiers, and X. Lu, ''Specialized Monte Carlo codes versus general-purpose Monte Carlo codes,'' American Nuclear Society, 2001 Winter Meeting, Accelerator Applications/Accelerator Driven Transmission Technology and Application (AccApp/ADTTA'01), November 11–15, Reno, Nevada, 2001.

[12] F. Salvat, J. M. Fernández-Varea, J. Baró, and J. Sempau, PENELOPE, an algorithm and computer code for Monte Carlo simulation of electron-photon showers, Informes Tecnicos CIEMAT Report No. 799, CIEMAT, Madrid, 1996.

[13] *Handbook on Photonuclear Data for Applications*, IAEA–TECDOC, March 2000 (International Atomic Energy Agency, Vienna, Austria, 2000).

[14] *MCNPX User's Guide*, edited by L. S. Waters (Los Alamos National Laboratory, Los Alamos, NM, 1999).

[15] E. Glatstein, ''The return of the snake oil salesman,'' Int. J. Radiat. Oncol., Biol., Phys. **55**, 561–562 (2003).